NANO LETTERS

Letter

pubs.acs.org/NanoLett

Direct Patterning of Colloidal Quantum-Dot Thin Films for Enhanced and Spectrally Selective Out-Coupling of Emission

Ferry Prins, David K. Kim, Jian Cui, Eva De Leo, Leo L. Spiegel, Kevin M. McPeak, and David J. Norris*

Optical Materials Engineering Laboratory, Department of Mechanical and Process Engineering, ETH Zurich, 8092 Zurich, Switzerland

Supporting Information

ABSTRACT: We report on a template-stripping method for the direct surface patterning of colloidal quantum-dot thin films to produce highly luminescent structures with feature sizes less than 100 nm. Through the careful design of high quality bull's-eye gratings we can produce strong directional beaming (10° divergence) with up to 6-fold out-coupling enhancement of spontaneous emission in the surface-normal direction. A transition to narrow single-mode lasing is observed in these same structures at thresholds as low as 120 μJ/cm^2. In addition, we demonstrate that these structures can be fabricated on flexible substrates. Finally, making use of the size-tunable character of colloidal quantum dots, we demonstrate spectrally selective out-coupling of light from mixed quantum-dot films. Our results provide a straightforward route toward significantly improved optical properties of colloidal quantum-dot assemblies.

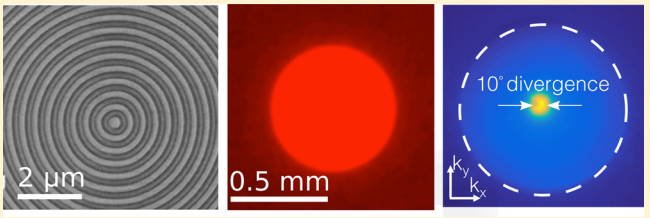

KEYWORDS: *Quantum dot, photonics, lasing, template stripping*

Colloidal quantum dots (cQDs), or semiconductor nanocrystals, are highly versatile building blocks that combine size-tunable optical properties with low-cost wet-chemical processing.[1,2] High quantum yields (>90%)[3] and spectrally narrow emission throughout the visible-near-infrared range[4] have placed cQDs among the highest color-quality emitters available, while at the same time outperforming most organic emitters in terms of photostability.[5] A number of cQD-based display[6,7] and lighting technologies[8−10] have recently emerged, while backlit display systems have already entered the market.[11] With internal conversion efficiencies of cQDs approaching unity, the light-extraction efficiencies from cQD films have become the limiting factor in terms of brightness. As is inherent to such high refractive-index layers, a significant portion of the emission undergoes internal reflection and gets trapped into waveguiding modes, leading to reabsorptive losses and reduced brightness. To overcome this issue, research efforts are increasingly shifting toward the development of nanophotonic light-management strategies that improve the out-coupling from these materials.

A number of successful photonic strategies for enhanced extraction of cQD emission have been developed recently. These include, for example, external out-coupling schemes in which the cQDs are coupled to plasmonic[12] or photonic-crystal[13] structures or are embedded in photonic microcavities.[14] While these external out-coupling schemes can provide strongly enhanced[15] and highly directional[12] extraction of cQD emission, it remains challenging to achieve these characteristics without significantly increasing the complexity of the overall system. A conceptually more straightforward approach would be to pattern the high refractive-index cQD film directly. Direct patterning of the light-emitting layer has been successfully applied in organic light-emitting polymers, for example, by structuring the surface with linear or circular Bragg gratings.[16,17]

Bragg scattering of waveguided light leads to constructive interference of emission in the out-of-plane direction when the in-plane momentum is conserved. The angle of out-coupling θ with respect to the surface normal for a given emission wavelength λ_{em} and a grating periodicity Λ is then governed by the Bragg condition, given by

$$k_0 \sin\theta = \pm k_{wg} \pm m k_g = \pm \frac{2\pi n_{eff}}{\lambda_{em}} \pm m\frac{2\pi}{\Lambda} \quad (1)$$

where k_0 is the wavevector of the outcoupled light, k_{wg} is the wavevector of the waveguided light, k_g is the Bragg vector, n_{eff} is the effective refractive index of the waveguide mode, and m is the diffraction order. Hence, first order diffraction allows waveguided light to scatter in the out-of-plane ($\theta = 0$) normal direction when $\lambda_{em} = \Lambda \cdot n_{eff}$. In a circularly symmetric bull's-eye grating, where momentum matching is satisfied for each radial direction, this results in a distinct beaming of fluorescence from the center of the structure.[18] Additionally, while the first-order diffraction couples the emission out vertically, the second-order diffraction can provide in-plane feedback, a concept that has been successfully employed to construct surface-emitting Bragg lasers.[19]

Received: August 2, 2016
Revised: December 6, 2016
Published: January 25, 2017

DOI: 10.1021/acs.nanolett.6b03212
Nano Lett. 2017, 17, 1319−1325

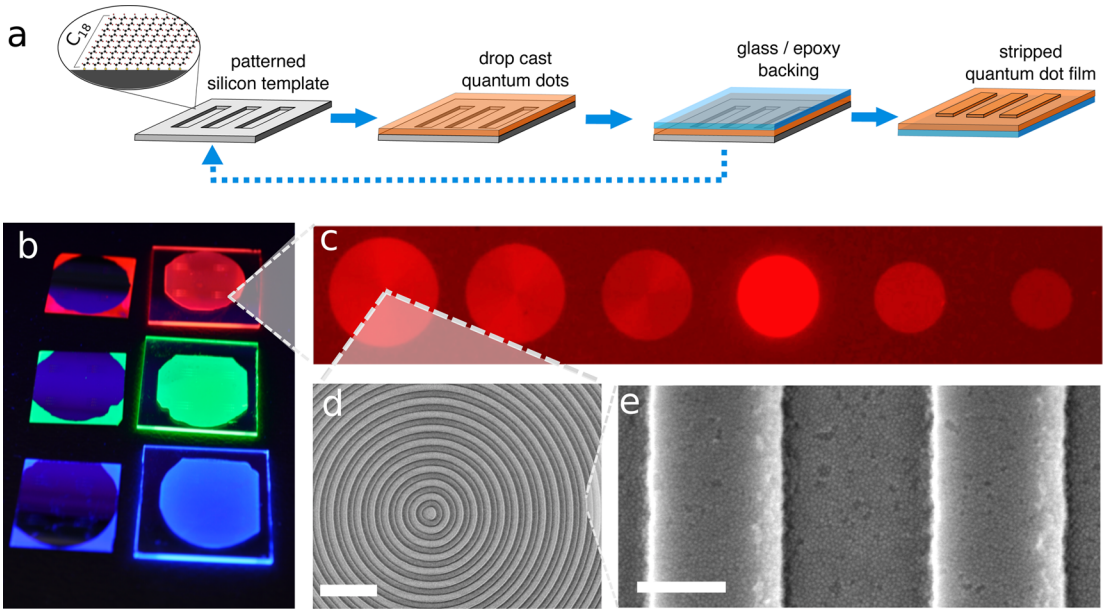

Figure 1. (a) Schematic of the template-stripping technique for fabricating surface-patterned cQD films. (b) Photograph of ultraviolet-illuminated patterned films of red-, green-, and blue-emitting cQDs that were fabricated using template stripping. On the left-hand side, the corresponding templates of 2 × 2 cm each are shown. (c) Fluorescence microscopy image of an array of bull's-eye gratings of 300 concentric circles each on a red-emitting cQD film. The pitch of these gratings varies from Λ = 550 nm on the left to Λ = 300 nm on the right with 50 nm decrements. (d,e) Scanning electron micrographs at different magnifications of a bull's-eye grating with a pitch of 550 nm. Scale bars are 2 μm and 200 nm.

The fabrication of Bragg gratings requires high-quality subwavelength patterning of the surface of the light-emitting film. In organic films, Bragg gratings have been fabricated using, for example, soft lithography or stamping.[16,19,20] Even though cQDs profit from many of the advantages of solution processability, few methods exist to produce patterned assemblies with submicron resolution.[21] Inkjet[22] and electrohydrodynamic[23] printing techniques have been developed to produce patterned films and are capable of achieving submicron resolution. However, the structural definition of taller structures is poor for these techniques, making them unsuitable for high-quality photonic Bragg gratings. Soft lithography and stamping techniques do exist for cQD solids,[7,24] but submicron resolution is challenging. In particular, the reduced structural cohesion of cQD solids as compared to most organic materials makes patterning of cQD solids using soft lithography more prone to pattern distortion. Pattern definition using electron beam lithography in combination with lift-off techniques would potentially allow for higher-resolution patterning of taller structures.[25] However, while such techniques have yielded patterned cQD films for electronic applications[25] photonic structuring has not yet been reported. Finally, alternative strategies for printing,[26] patterning,[27] and soft-lithography[28,29] have been developed using matrix-embedded cQD films, though the use of such composite films has the distinct disadvantage of diluted emitter concentration, which inevitably places limitations on the emission intensity.

Here, we present a new methodology for the direct patterning of cQD assemblies using template stripping, yielding significant improvements in the out-coupling efficiency of cQD emission using surface-patterned bull's eye gratings. Our fabrication method is similar to template stripping techniques used to fabricate patterned metal films[30] and macroscale assemblies of plasmonic nanoparticles.[31] Figure 1a shows a schematic of the process. Patterned silicon templates are fabricated using standard electron-beam lithography and reactive ion etching and are subsequently coated with a self-assembled monolayer using a previously reported[32,33] octadecyltrichlorosilane (ODTS) treatment (see Methods for details). The cQDs are then drop-cast onto the template to form a dense and continuous layer. In the next step, a glass backing substrate is attached to the colloidal film using an ultraviolet-curable epoxy. In a final step, the colloidal film is mechanically peeled off the template to expose the patterned surface defined by the template. The template can be reused after a simple cleaning procedure. The use of the high-quality self-assembled monolayer on the silicon template is essential to the success of this technique. Template stripping relies on a well-defined "weakest link" in the layer stack. Without the self-assembled monolayer, the adhesion between the cQDs and the template would be competing with the cQD−cQD adhesion in the film itself.[7] Using our technique, lateral feature sizes as small as 100 nm are achievable, while feature heights as tall as 100 nm were reproducibly obtained (see Supporting Information).

Making use of the size-tunable character of the quantum dots, films of different colors can be prepared. Figure 1b shows a photograph of ultraviolet-illuminated patterned films of red-emitting CdSe/CdZnS (λ_{em} = 622 nm), green-emitting CdSe/CdZnS (λ_{em} = 526 nm), and blue-emitting CdS/ZnS (λ_{em} = 460 nm) core/shell cQDs that were fabricated using template stripping. On the left-hand side, the corresponding templates of the three films are shown. The absence of fluorescence from the central region of the template demonstrates that the films are stripped completely. The pattern transfer is highly uniform across large areas and shows high fidelity down to the submicron level, as is evidenced by both fluorescence microscopy imaging (Figure 1c) and high-resolution scanning electron microscopy (Figure 1d,e) of bull's-eye grating structures at the surface of a red-emitting cQD film.

The bull's-eye gratings shown in Figure 1c show a clear pitch-dependent intensity of the spontaneous emission. The substrate contains an array of gratings, each with 300 concentric circles

DOI: 10.1021/acs.nanolett.6b03212
Nano Lett. 2017, 17, 1319−1325

and a 50% fill factor. These structures are patterned onto the surface of a 50 nm thick red-emitting cQD film (λ_{em} = 622 nm). From left to right, the grating pitch varies from Λ = 550 to 300 nm with 50 nm decrements. The brightest emission in the low numerical aperture image (N.A. = 0.06) is observed for the circular grating with a pitch of Λ = 400 nm, indicative of Bragg scattering of waveguided light along the surface normal. Before discussing the out-coupling enhancement and the improved brightness of our films, we first focus on the angular dependence of the Bragg scattering for the different pitches.

To obtain more insight into the angular dependence of the emission from the different bull's-eye gratings, we performed k-space imaging with high numerical aperture (N.A. = 0.8) light collection. Normalized k-space color maps taken at the center of the bull's-eye gratings of different pitches (Λ between 500 and 300 nm) are shown in Figure 2a, and vertical line traces

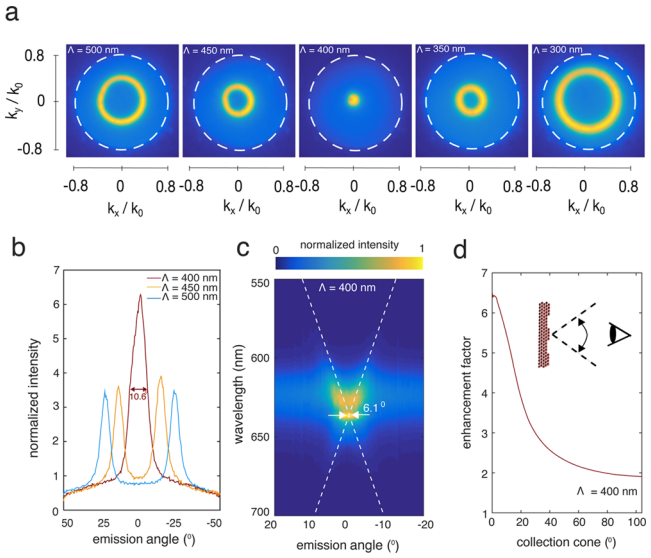

Figure 2. (a) Normalized *k*-space color maps of fluorescent emission from the right-most five bull's-eye gratings of Figure 1c (Λ = 500−300 nm). Dashed white lines indicate the numerical aperture of the objective (N.A. = 0.8). (b) Vertical line traces at k_x/k_0 = 0 through the *k*-space color maps of the left most three panels of panel a (Λ = 500, 450, and 400 nm). Traces are normalized to the maximum nonresonant intensity. (c) Normalized spectral-angular color map of the Λ = 400 nm bull's eye grating. Dashed white lines are fits to eq 1 (see text for details). (d) Enhancement of fluorescence out-coupling from the Λ = 400 nm bull's eye grating as compared to the nonresonant case, as a function of the collection cone (see inset for schematic).

across the center of the k-space maps are shown in Figure 2b (for Λ = 400, 450, and 500 nm). Indeed, the enhanced emission for the bull's-eye grating with pitch Λ = 400 nm is centered at small k-vectors, indicating fluorescent beaming in the surface-normal direction. The resonant out-coupling occurs at different angles for both smaller and larger pitches, resulting in the observed donut-like emission patterns in k-space, with the pitch dependence of the angle of out-coupling following the Bragg condition given by eq 1 (see Figure S2). From the full-width-at-half-maximum (fwhm) of the Λ = 400 nm line-trace in Figure 2b we measure the divergence of the beam to be 10.6°.

The width of the divergence is partially a result of spectral broadening of the resonance. The full spectral-angular response of the Λ = 400 nm bull's eye grating is shown in Figure 2c. This spectral−angular color map is obtained by dispersing the *k*-space line trace of Figure 2b using an imaging spectrograph. Despite the narrow emission line width of the cQD ensemble, it is clear that distinct variations in the emission angle are present across the width of the emission spectrum. The shifting of the resonance as a function of wavelength can be fitted to eq 1, using the effective refractive index (n_{eff}) of the waveguided mode as the only fit parameter. Good agreement is found for n_{eff} = 1.6 ± 0.1, as can be seen from the dashed white lines in Figure 2c. This value for n_{eff} is reasonable considering the sample geometry and the refractive index of our cQD material (n = 1.8), as confirmed by simulations of the photonic band structure (see Figure S3). At the point of narrowest divergence, located at 638 nm, the divergence measures a fwhm of 6.1°. It is interesting to note that this value for spectrally resolved divergence approaches those reported for cQD ensembles coupled to circular plasmonic gratings, where a divergence of 3.5−4.5° was recently reported.[34,35]

Aside from controlling the directionality of emission, our simple surface patterning strategy dramatically enhances the overall brightness of the cQD films. To quantify this, we compare the angular emission profile from the Λ = 400 nm bull's-eye grating (see red line in Figure 2b) with the experimentally obtained angular emission profile from the nonresonant background. The out-coupling enhancement factor as a function of the collection cone is shown in Figure 2d. Integrated over a wide collection cone (>100°), our patterned film emits almost twice as much as compared to the unpatterned case. Moreover, in the direct out-of-plane direction, the strong beaming effect results in over 6-fold enhancement of out-coupling. It is important to note that these values are hemispherical enhancement factors. Further improvements in the directionality can be achieved using for example back reflectors (see Figure S5).

Beyond the out-coupling enhancement of spontaneous emission, our bull's-eye gratings also enable significantly improved stimulated emission characteristics. As previously mentioned, Bragg grating structures can provide both enhanced out-coupling through the first-order diffraction, as well as feedback in the in-plane direction through second-order diffraction. To promote efficient in-plane feedback, we have fabricated bull's-eye gratings using slightly thicker films (100 nm) to provide better confinement of the waveguide mode. Indeed, under increasing excitation power we observe a clear transition from spontaneous emission to stimulated emission. This transition is characterized by a distinct spectral narrowing and sharp increase in the output power of the emission, an example of which is shown in Figure 3a for a red-emitting Λ = 374 nm bull's-eye grating. The spectral narrowing results in a single-mode emission peak at 638 nm (n_{eff} = 1.7) with a line-width of 0.7 nm (2 meV) and a total intensity increase of over an order of magnitude before reaching saturation (see inset of Figure 3a). Spectral changes are accompanied by a reduction in the beam divergence from around 10° (174 mrad) for spontaneous emission down to 0.6° (10 mrad) for lasing, as can be seen from the *k*-space map in Figure 3b. The lasing from these structures exhibits low thresholds, consistently below 150 $\mu J/cm^2$ and in some cases as low as 110 $\mu J/cm^2$. These thresholds are comparable to those obtained using more complex microcavity structures or external distributed feedback schemes.[29,36,37] Low-threshold lasing is indicative of efficient in-plane feedback and low-loss waveguiding and is

DOI: 10.1021/acs.nanolett.6b03212
Nano Lett. 2017, 17, 1319−1325

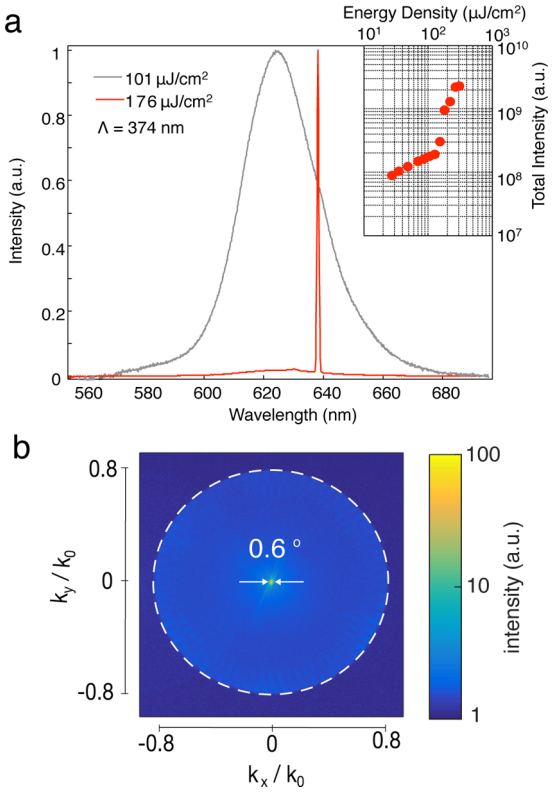

Figure 3. (a) Normalized emission spectra of a red-emitting Λ = 374 nm bull's-eye grating below (gray line) and above (red line) the stimulated emission threshold. Inset: Total emission intensity as a function of energy density of the pump excitation, showing a clear threshold for stimulated emission at 120 $\mu J/cm^2$ for this structure. (b) *k*-space color map on a logarithmic intensity scale of the emission of a bull's-eye grating above the lasing threshold, indicating the fwhm divergence of 0.6°. Dashed white lines indicate the numerical aperture of the objective (N.A. = 0.8).

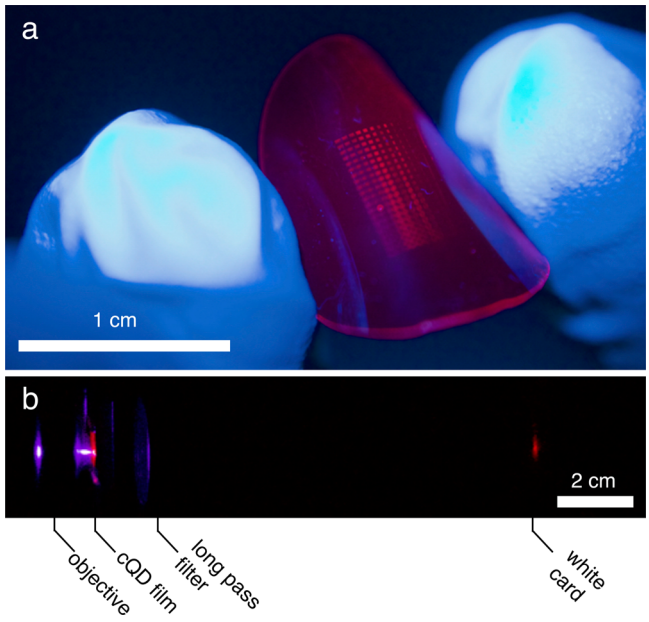

Figure 4. (a) Photograph of an ultraviolet-illuminated flexible film of red-emitting cQDs with an array of surface-patterned gratings. (b) Photograph of the lasing beam emitted from a bull's-eye grating (Λ = 374 nm) on the flexible film when illuminated above lasing threshold (210 $\mu J/cm^2$).

therefore a further confirmation of the high structural fidelity of our patterned films.

An interesting aspect of the template stripping method is the ability to release the epoxy layer together with the patterned cQD film from the glass substrate using a razor blade. The resulting freestanding flexible structure (Figure 4a) maintains the optical characteristics in terms of enhanced out-coupling as well as distributed feedback lasing. To demonstrate this, we illuminate one of the bull's-eye gratings on a flexible substrate above the lasing threshold and project the resulting beam onto a white card, as is shown in Figure 4b. Consistent with the highly directional emission from these structures, a clear circular beam with a Gaussian profile is observed. Whereas earlier reports of flexible cQD lasers required relatively high pump fluences,[38−40] our template stripping method provides a straightforward route to low-threshold, single mode, and flexible lasing sources that may further facilitate their application in spectroscopic assays, as well as future projection and display technologies.[41]

As a final demonstration of the versatility of the template stripping method, we fabricated bull's eye gratings with different pitches onto a mixed red-green-blue (RGB) cQD film to provide color tuning of spontaneous emission through spectrally selective out-coupling. This combined spectral tunability of both the cQD building block as well as the photonic grating structure is a unique feature of our wavelength-scale patterned of cQD films. A fluorescence image of the resulting structures is shown in Figure 5a. The emission from the unpatterned film in the background consists of a mix of the three individual colors to make up the spectrum displayed in Figure 5b. Each of the patterned Bragg gratings enhances a select portion of the emission spectrum of the mixed film in the surface-normal direction, leading to the varying colors observed in Figure 5a and the corresponding spectra shown in Figure 5b. Effectively, the different patterns shift the color gamut of the out-coupled light from the mixed RGB film (see Supporting Information for more details). The green and red color channels are most widely tunable, whereas tuning of blue channel is less effective. This is perhaps not surprising because the higher energy blue emission in the mixed film experiences more losses due to reabsorption by red and green dots. Reabsorption leads to reduced waveguiding, less interference, and thus less enhancement of the out-coupling through the first-order Bragg diffraction. A potential solution to reabsorption losses is to use Stoke-shift engineered cQDs,[42] where significant absorption for each color only occurs at wavelengths shorter than 450 nm (i.e., at energies above the blue emission spectrum). Nevertheless, as shown in Figure 5b, significant color shifts can be achieved for the different Bragg patterns with the current mixed films.

The demonstrated spatially and spectrally selective out-coupling of emission provides new levels of control over the optical properties of cQD assemblies. While previous strategies required complex photonic crystal[13] or plasmonic[43] structures to achieve such photonic control, the presented method of high-resolution direct patterning provides a straightforward and cost-effective route toward flexible devices with enhanced and directional out-coupling of emission. In particular, the out-coupling enhancement of spontaneous and stimulated emission from patterned films has direct technological relevance in the use of cQD assemblies in optical down-conversion for backlight displays,[11] LEDs,[6] and single-mode surface-emitting lasers.[41]

DOI: 10.1021/acs.nanolett.6b03212
Nano Lett. 2017, 17, 1319−1325

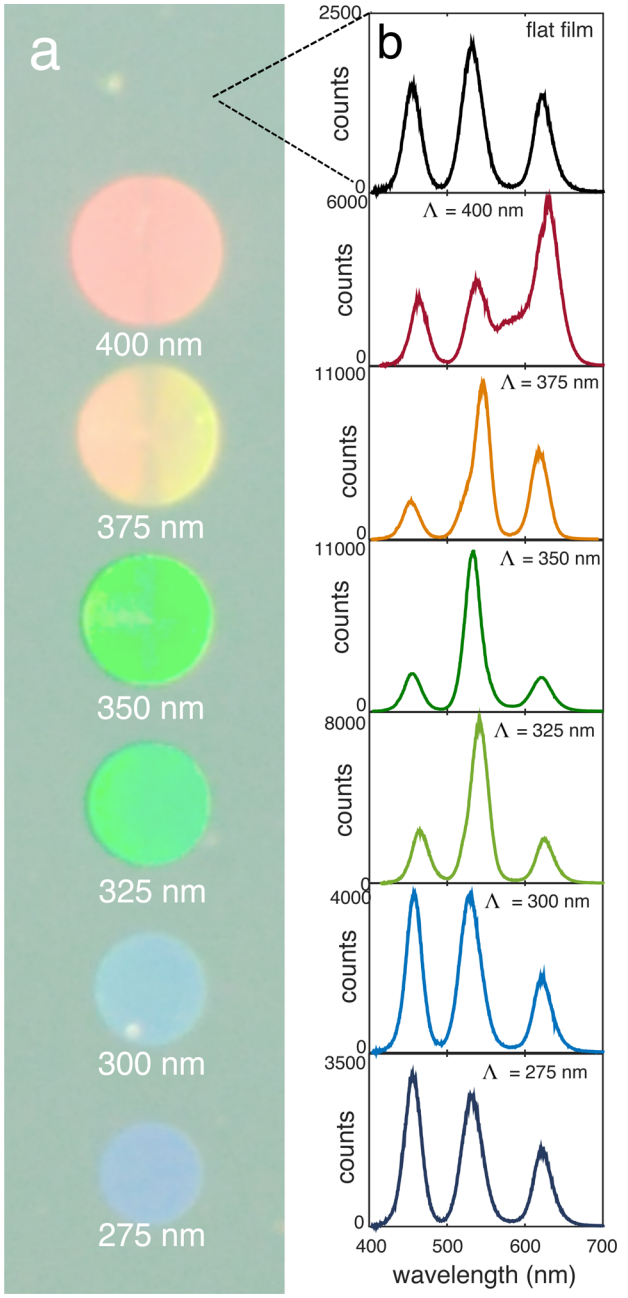

Figure 5. (a) Fluorescence microscopy image of an array of bull's-eye gratings patterned into a RGB-emitting mixed cQD film with 300 rings each and a pitch decreasing from top to bottom in 25 nm steps from Λ = 400−275 nm. (b) Emission spectra of the unpatterned and patterned RGB-emitting mixed cQD film (N.A. = 0.2).

Methods. *Template Fabrication.* Patterned silicon (100) templates were fabricated using standard e-beam lithography and reactive ion etching techniques (see Supporting Information for details). Patterned templates were cleaned using O_2 plasma (600W, 3 min.) and piranha treatment (1:1 H_2O_2/H_2SO_4, 15 min.). The templates were subsequently coated with a dense self-assembled monolayer (SAM) using a previously reported octadecyltrichlorosilane treatment.[32] The resulting hydrophobic surface yields a contact angle >110°.

Template Stripping. Red-emitting CdSe/CdZnS (λ_{em} = 622 nm), green-emitting CdSe/CdZnS (λ_{em} = 526 nm), and blue-emitting CdS/ZnS (λ_{em} = 460 nm) core−shell quantum dots were synthesized based on previously reported procedures (see Supporting Information for details).[44−47] All three cQD systems have a comparable total core−shell particle diameter of approximately 10−12 nm. Special care was taken in the isolation of the quantum dots to remove unreacted material and excess ligands, since this significantly improves the homogeneity of drop casting in the following step and the ability to clean the templates for future use. cQDs were drop-cast from 9:1 hexane/octane solutions with optical densities (1 cm optical path length) at the first excitonic peak of 2.0 (red and blue) and 6.0 (green), using 35 μL for a 20 × 20 mm template size. Mixed RGB films were prepared using a ratio of 1:3:15 of red, green, and blue solutions in 9:1 hexane/octane of before mentioned optical densities. Using these drop-cast conditions, a cQD backing-layer of ∼50 nm thickness is formed on top of the patterns. Red-emitting films for lasing were prepared from a solution with an optical density of 4.0 to achieve thicker backing-layers of ∼100 nm for improved feedback of the waveguided mode. Template stripping was performed by placing a drop of epoxy (NOA 61, Norland Products) on the cQD film after drying and gently placing a glass slide on top. The epoxy was allowed to flow toward the edges of the template until only the corners were free, after which it was cured with a 365 nm UV lamp for 30 min. After curing, the silicon template was separated from the cQD/epoxy/glass stack by placing a razor blade between the silicon template and the glass slide at one of the corners of the template, thereby exposing the patterned cQD film. For freestanding flexible films of cQDs on epoxy, a razor blade was used to separate the epoxy layer from the glass slide. Templates can be cleaned for future use through ultrasonication in chloroform for 5 min. The SAM maintains sufficient quality for 10−15 drop casts, although best results are generally obtained with freshly prepared SAMs. An O_2 plasma (600 W, 10 min) and piranha treatment (1:1 H_2O_2/H_2SO_4, 15 min.) can be used to remove the SAM, making the template ready for a new octadecyltrichlorosilane treatment.

Fluorescence Microscopy. Optical characterization was performed using an inverted microscope (Nikon, TE200) equipped with a high-pressure mercury lamp (365 nm excitation). Fluorescence was collected using a 2× (N.A. 0.06) or 10× objective (N.A. 0.2), relay optics (focal length of f = 100 mm) and an imaging spectrograph (Horiba, Triax 320, 150 gr/mm grating) equipped with a nitrogen-cooled CCD detector (Princeton Instruments, Spec-10). Fluorescence microscopy images were recorded using a Nikon D3200 digital camera (white balance 3500K). For k-space imaging, fluorescence was collected using a 50× objective (Nikon, TU Plan Fluor, N.A. 0.8) and a 60 mm Fourier lens was used to project the back aperture of the objective onto the entrance slit of the imaging spectrograph. The k-space color maps were recorded using a fully opened slit and zero dispersion. Spectral-angular color maps were recorded using a 25 μm slit opening and spectral dispersion using a 150 gr/mm grating.

Lasing Experiments. The 450 nm pulses (∼340 fs pulse duration, 1 kHz repetition rate) were generated by a collinear optical parametric amplifier (Spectra-Physics, Spirit-OPA) pumped by a 1040 nm pump laser (Spectra-Physics, Spirit-1040-8). After appropriate spectral filtering, the beam was directed through a gradient neutral density filter wheel to adjust the pulse power (Thorlabs, NDC-50C-2M-B). After beam expansion and collimation, a small portion of the beam was directed to a photodiode to monitor the pump power (Thorlabs, DET110). The rest of the beam was passed through

DOI: 10.1021/acs.nanolett.6b03212
Nano Lett. 2017, 17, 1319−1325

a defocusing lens (f = 150 mm) into an inverted microscope (Nikon, Eclipse Ti-U). The beam was then directed upward to the sample using a 488 nm long pass dichroic beamsplitter through a 50× air objective (Nikon, TU Plan Fluor, N.A. 0.8). The defocusing lens was adjusted to provide a spot size of ∼90 um. The spot size was determined from the image of the photoluminescence from a flat portion of a film of template-stripped cQDs. To best approximate the defocused intensity profile, the cross-section of the spot was fitted with the sum of two Gaussian functions and the full width at half-maximum was determined numerically. The excitation power density at the sample was monitored by correlating the power meter reading above the objective at the sample plane (Thorlabs, S170C with PM100D) with the current reading from the photodiode. Photoluminescence from the sample was collected by the same objective and directed through the dichroic beamsplitter, a 500 nm long pass emission filter, and relay lenses (f = 200 mm) into an imaging spectrometer (Andor, Shamrock 303i). For k-space imaging of the lasing, the lens for focusing into the spectrometer was replaced by a combination of an f = 50 mm lens and an f = 60 mm lens. The photoluminescence was dispersed with a 300 lines/mm grating (500 nm blaze) and imaged with an air-cooled electron-multiplying CCD camera (Andor, iXon 888 Ultra).

■ ASSOCIATED CONTENT

Supporting Information

The Supporting Information is available free of charge on the ACS Publications website at DOI: 10.1021/acs.nanolett.6b03212.

A detailed discussion on the experimental methods and analysis (PDF)

■ AUTHOR INFORMATION

Corresponding Author

*E-mail: dnorris@ethz.ch (D.J.N.). Fax: +41 44 632 10 23.

ORCID

Ferry Prins: 0000-0001-7605-1566

Present Addresses

(D.K.K.) MIT Lincoln Laboratory, Lexington, MA.
(K.M.M.) Cain Department of Chemical Engineering, Louisiana State University, Baton Rouge, LA.

Author Contributions

F.P. and D.K.K. contributed equally.

Notes

The authors declare no competing financial interest.

■ ACKNOWLEDGMENTS

We gratefully acknowledge funding from the European Research Council under the European Union's Seventh Framework Program (FP/2007-2013)/ERC Grant 339905 (QuaDoPS Advanced Grant). F.P. acknowledges support by the Ambizione program of the Swiss National Science Foundation. J.C. acknowledges funding from the ETH Zurich Postdoctoral Fellowship Program and the Marie Curie Actions for People COFUND Program. We thank B. le Feber and J. Winkler for discussions. We thank Y. Fedoryshyn, A. Olziersky, U. Drechsler, and M. Sousa for assistance in the fabrication and characterization.

■ REFERENCES

(1) Alivisatos, A. P. Semiconductor Clusters, Nanocrystals, and Quantum Dots. *Science* **1996**, *271*, 933−937.
(2) Kim, J. Y.; Voznyy, O.; Zhitomirsky, D.; Sargent, E. H. 25th Anniversary Article: Colloidal Quantum Dot Materials and Devices: A Quarter-Century of Advances. *Adv. Mater.* **2013**, *25*, 4986−5010.
(3) Chen, O.; Zhao, J.; Chauhan, V. P.; Cui, J.; Wong, C.; Harris, D. K.; Wei, H.; Han, H.-S.; Fukumura, D.; Jain, R. K.; et al. Compact high-quality CdSe-CdS core-shell nanocrystals with narrow emission linewidths and suppressed blinking. *Nat. Mater.* **2013**, *12*, 445−451.
(4) Murray, C. B.; Norris, D. J.; Bawendi, M. G. Synthesis and characterization of nearly monodisperse CdE (E = sulfur, selenium, tellurium) semiconductor nanocrystallites. *J. Am. Chem. Soc.* **1993**, *115*, 8706−8715.
(5) Shirasaki, Y.; Supran, G. J.; Bawendi, M. G.; Bulović, V. Emergence of colloidal quantum-dot light-emitting technologies. *Nat. Photonics* **2012**, *7*, 13−23.
(6) Jang, E.; Jun, S.; Jang, H.; Lim, J.; Kim, B.; Kim, Y. White-light-emitting diodes with quantum dot color converters for display backlights. *Adv. Mater.* **2010**, *22*, 3076−3080.
(7) Kim, T.-H.; Cho, K.-S.; Lee, E. K.; Lee, S. J.; Chae, J.; Kim, J. W.; Kim, D. H.; Kwon, J.-Y.; Amaratunga, G.; Lee, S. Y.; et al. Full-colour quantum dot displays fabricated by transfer printing. *Nat. Photonics* **2011**, *5*, 176−182.
(8) Colvin, V. L.; Schlamp, M. C.; Alivisatos, A. P. Light-emitting diodes made from cadmium selenide nanocrystals and a semiconducting polymer. *Nature* **1994**, *370*, 354−357.
(9) Anikeeva, P. O.; Halpert, J. E.; Bawendi, M. G.; Bulović, V. Quantum Dot Light-Emitting Devices with Electroluminescence Tunable over the Entire Visible Spectrum. *Nano Lett.* **2009**, *9*, 2532−2536.
(10) Shirasaki, Y.; Supran, G. J.; Bawendi, M. G.; Bulović, V. Emergence of colloidal quantum-dot light-emitting technologies. *Nat. Photonics* **2012**, *7*, 13−23.
(11) Bourzac, K. Quantum dots go on display. *Nature* **2013**, *493*, 283.
(12) Curto, A. G.; Volpe, G.; Taminiau, T. H.; Kreuzer, M. P.; Quidant, R.; van Hulst, N. F. Unidirectional emission of a quantum dot coupled to a nanoantenna. *Science* **2010**, *329*, 930−933.
(13) Lodahl, P.; Floris Van Driel, A.; Nikolaev, I. S.; Irman, A.; Overgaag, K.; Vanmaekelbergh, D.; Vos, W. L. Controlling the dynamics of spontaneous emission from quantum dots by photonic crystals. *Nature* **2004**, *430*, 654−657.
(14) Poitras, C. B.; Lipson, M.; Du, H.; Hahn, M. A.; Krauss, T. D. Photoluminescence enhancement of colloidal quantum dots embedded in a monolithic microcavity. *Appl. Phys. Lett.* **2003**, *82*, 4032.
(15) Hoang, T. B.; Akselrod, G. M.; Argyropoulos, C.; Huang, J.; Smith, D. R.; Mikkelsen, M. H. Ultrafast spontaneous emission source using plasmonic nanoantennas. *Nat. Commun.* **2015**, *6*, 7788.
(16) Matterson, B. J.; Lupton, J. M.; Safonov, A. F.; Salt, M. G.; Barnes, W. L.; Samuel, I. D. W. Increased Efficiency and Controlled Light Output from a Microstructured Light-Emitting Diode. *Adv. Mater.* **2001**, *13*, 123−127.
(17) Lupton, J. M.; Matterson, B. J.; Samuel, I. D. W.; Jory, M. J.; Barnes, W. L. Bragg scattering from periodically microstructured light emitting diodes. *Appl. Phys. Lett.* **2000**, *77*, 3340.
(18) Erdogan, T.; Hall, D. G. Circularly symmetric distributed feedback semiconductor laser: An analysis. *J. Appl. Phys.* **1990**, *68*, 1435.
(19) Jebali, A.; Mahrt, R. F.; Moll, N.; Erni, D.; Bauer, C.; Bona, G.-L.; Bächtold, W. Lasing in organic circular grating structures. *J. Appl. Phys.* **2004**, *96*, 3043.
(20) Ziebarth, J. M.; Saafir, A. K.; Fan, S.; McGehee, M. D. Extracting Light from Polymer Light-Emitting Diodes Using Stamped Bragg Gratings. *Adv. Funct. Mater.* **2004**, *14*, 451−456.
(21) Yang, J.; Choi, M. K.; Kim, D.-H.; Hyeon, T. Designed Assembly and Integration of Colloidal Nanocrystals for Device Applications. *Adv. Mater.* **2016**, *28*, 1176−1207.

DOI: 10.1021/acs.nanolett.6b03212
Nano Lett. 2017, 17, 1319−1325

(22) Wood, V.; Panzer, M. J.; Chen, J.; Bradley, M. S.; Halpert, J. E.; Bawendi, M. G.; Bulović, V. Inkjet-Printed Quantum Dot-Polymer Composites for Full-Color AC-Driven Displays. *Adv. Mater.* **2009**, *21*, 2151−2155.
(23) Kress, S. J. P.; Richner, P.; Jayanti, S. V.; Galliker, P.; Kim, D. K.; Poulikakos, D.; Norris, D. J. Near-field light design with colloidal quantum dots for photonics and plasmonics. *Nano Lett.* **2014**, *14*, 5827−5833.
(24) Kim, L.; Anikeeva, P. O.; Coe-Sullivan, S. A.; Steckel, J. S.; Bawendi, M. G.; Bulović, V. Contact printing of quantum dot light-emitting devices. *Nano Lett.* **2008**, *8*, 4513−4517.
(25) Mentzel, T. S.; Wanger, D. D.; Ray, N.; Walker, B. J.; Strasfeld, D.; Bawendi, M. G.; Kastner, M. A. Nanopatterned electrically conductive films of semiconductor nanocrystals. *Nano Lett.* **2012**, *12*, 4404−4408.
(26) Kim, J. Y.; Ingrosso, C.; Fakhfouri, V.; Striccoli, M.; Agostiano, A.; Curri, M. L.; Brugger, J. Inkjet-Printed Multicolor Arrays of Highly Luminescent Nanocrystal-Based Nanocomposites. *Small* **2009**, *5*, 1051−1057.
(27) Tamborra, M.; Striccoli, M.; Curri, M. L.; Alducin, J. A.; Mecerreyes, D.; Pomposo, J. A.; Kehagias, N.; Reboud, V.; Sotomayor Torres, C. M.; Agostiano, A. Nanocrystal-Based Luminescent Composites for Nanoimprinting Lithography. *Small* **2007**, *3*, 822−828.
(28) Sundar, V. C.; Eisler, H.-J.; Deng, T.; Chan, Y.; Thomas, E. L.; Bawendi, M. G. Soft-Lithographically Embossed, Multilayered Distributed-Feedback Nanocrystal Lasers. *Adv. Mater.* **2004**, *16*, 2137−2141.
(29) Todescato, F.; Fortunati, I.; Gardin, S.; Garbin, E.; Collini, E.; Bozio, R.; Jasieniak, J. J.; Della Giustina, G.; Brusatin, G.; Toffanin, S.; et al. Soft-Lithographed Up-Converted Distributed Feedback Visible Lasers Based on CdSe-CdZnS-ZnS Quantum Dots. *Adv. Funct. Mater.* **2012**, *22*, 337−344.
(30) Nagpal, P.; Lindquist, N. C.; Oh, S.-H.; Norris, D. J. Ultrasmooth patterned metals for plasmonics and metamaterials. *Science* **2009**, *325*, 594−597.
(31) Alba, M.; Pazos-Perez, N.; Vaz, B.; Formentin, P.; Tebbe, M.; Correa-Duarte, M. A.; Granero, P.; Ferré-Borrull, J.; Alvarez, R.; Pallares, J.; et al. Macroscale Plasmonic Substrates for Highly Sensitive Surface-Enhanced Raman Scattering. *Angew. Chem., Int. Ed.* **2013**, *52*, 6459−6463.
(32) Lessel, M.; Bäumchen, O.; Klos, M.; Hähl, H.; Fetzer, R.; Paulus, M.; Seemann, R.; Jacobs, K. Self-assembled silane monolayers: an efficient step-by-step recipe for high-quality, low energy surfaces. *Surf. Interface Anal.* **2015**, *47*, 557−564.
(33) McPeak, K. M.; van Engers, C. D.; Bianchi, S.; Rossinelli, A.; Poulikakos, L. V.; Bernard, L.; Herrmann, S.; Kim, D. K.; Burger, S.; Blome, M.; et al. Ultraviolet Plasmonic Chirality from Colloidal Aluminum Nanoparticles Exhibiting Charge-Selective Protein Detection. *Adv. Mater.* **2015**, *27*, 6244−6250.
(34) Harats, M. G.; Livneh, N.; Zaiats, G.; Yochelis, S.; Paltiel, Y.; Lifshitz, E.; Rapaport, R. Full spectral and angular characterization of highly directional emission from nanocrystal quantum dots positioned on circular plasmonic lenses. *Nano Lett.* **2014**, *14*, 5766−5771.
(35) Livneh, N.; Harats, M. G.; Yochelis, S.; Paltiel, Y.; Rapaport, R. Efficient Collection of Light from Colloidal Quantum Dots with a Hybrid Metal−Dielectric Nanoantenna. *ACS Photonics* **2015**, *2*, 1669−1674.
(36) Dang, C.; Lee, J.; Breen, C.; Steckel, J. S.; Coe-Sullivan, S.; Nurmikko, A. Red, green and blue lasing enabled by single-exciton gain in colloidal quantum dot films. *Nat. Nanotechnol.* **2012**, *7*, 335−339.
(37) Roh, K.; Dang, C.; Lee, J.; Chen, S.; Steckel, J. S.; Coe-Sullivan, S.; Nurmikko, A. Surface-emitting red, green, and blue colloidal quantum dot distributed feedback lasers. *Opt. Express* **2014**, *22*, 18800−18806.
(38) Menon, V. M.; Luberto, M.; Valappil, N. V.; Chatterjee, S. Lasing from InGaP quantum dots in a spin-coated flexible microcavity. *Opt. Express* **2008**, *16*, 19535.
(39) Chen, Y.; Guilhabert, B.; Herrnsdorf, J.; Zhang, Y.; Mackintosh, A. R.; Pethrick, R. A.; Gu, E.; Laurand, N.; Dawson, M. D. Flexible distributed-feedback colloidal quantum dot laser. *Appl. Phys. Lett.* **2011**, *99*, 241103.
(40) Foucher, C.; Guilhabert, B.; Laurand, N.; Dawson, M. D. Wavelength-tunable colloidal quantum dot laser on ultra-thin flexible glass. *Appl. Phys. Lett.* **2014**, *104*, 141108.
(41) Nurmikko, A. What future for quantum dot-based light emitters? *Nat. Nanotechnol.* **2015**, *10*, 1001−1004.
(42) Coropceanu, I.; Bawendi, M. G. Core/shell quantum dot based luminescent solar concentrators with reduced reabsorption and enhanced efficiency. *Nano Lett.* **2014**, *14*, 4097−4101.
(43) Livneh, N.; Strauss, A.; Schwarz, I.; Rosenberg, I.; Zimran, A.; Yochelis, S.; Chen, G.; Banin, U.; Paltiel, Y.; Rapaport, R. Highly directional emission and photon beaming from nanocrystal quantum dots embedded in metallic nanoslit arrays. *Nano Lett.* **2011**, *11*, 1630−1635.
(44) Reiss, P.; Bleuse, J.; Pron, A. Highly Luminescent CdSe/ZnSe Core/Shell Nanocrystals of Low Size Dispersion. *Nano Lett.* **2002**, *2*, 781−784.
(45) Boldt, K.; Kirkwood, N.; Beane, G. A.; Mulvaney, P. Synthesis of Highly Luminescent and Photo-Stable, Graded Shell CdSe/Cd x Zn 1− x S Nanoparticles by In Situ Alloying. *Chem. Mater.* **2013**, *25*, 4731−4738.
(46) Bae, W. K.; Char, K.; Hur, H.; Lee, S. Single-Step Synthesis of Quantum Dots with Chemical Composition Gradients. *Chem. Mater.* **2008**, *20*, 531−539.
(47) Lee, K.-H.; Lee, J.-H.; Song, W.-S.; Ko, H.; Lee, C.; Lee, J.-H.; Yang, H. Highly efficient, color-pure, color-stable blue quantum dot light-emitting devices. *ACS Nano* **2013**, *7*, 7295−7302.

DOI: 10.1021/acs.nanolett.6b03212
Nano Lett. 2017, 17, 1319−1325